Experimental evaluation of the partial thermal energy compensation of hydrate crystallization from cyclopentane-loaded porous activated carbon particles immersed in brine

Rafik Mallek, Christelle Miqueu, Matthieu Jacob, Christophe Dicharry

Experimental evaluation of the partial thermal energy compensation of hydrate crystallization from cyclopentane-loaded porous activated carbon particles immersed in brine

Rafik Mallek,[1] Christelle Miqueu,[2] Matthieu Jacob,[3] Christophe Dicharry[1,*]

[1] *CNRS/TOTAL/UNIV PAU & PAYS ADOUR, Laboratoire des Fluides Complexes et leurs Réservoirs - IPRA, UMR5150, 64000, Pau, France.*

[2] *CNRS/TOTAL/UNIV PAU & PAYS ADOUR, Laboratoire des Fluides Complexes et leurs Réservoirs - IPRA, UMR5150, 64600, Anglet, France.*

[3] *Pôle d'Etude et de Recherche de Lacq (PERL), TOTAL SA, 64170 Lacq, France.*

[*]Corresponding author(s): christophe.dicharry@univ-pau.fr (C. Dicharry)

Abstract

Hydrate-based desalination (HBD) is a potential water desalination technology that has been studied over the past decades. Recently, an HBD process based on hydrate formation from cyclopentane (CP) loaded on porous activated carbon particles (PACP) was patented ("Method for crystallizing clathrate hydrates, and method for purifying an aqueous liquid using the clathrate hydrates thus crystallized", EP3153606, 2017). It is thought that the crystallization of CP hydrates from CP adsorbed on PACP might cause partial thermal energy compensation. Actually, the heat released by the exothermic hydrate crystallization should be partially balanced by the endothermic desorption of CP from the PACP. In order to investigate this phenomenon, calorimetric and optical studies (heat flow and refractive index measurements respectively) of hydrate formation in systems consisting of CP-saturated PACP immersed in brines (3.5 wt% NaCl and 8 wt% NaCl) were performed. Comparison of the thermal energy measured directly (through the calorimetric study) - i.e. the energy produced by both hydrate crystallization and CP desorption - and the thermal energy measured

indirectly (deduced from the optical study) - i.e. the energy generated by hydrate crystallization only - revealed a balanced energy ranging from 9 to 47 kJ/mol of CP. Comparison of the latter with the differential enthalpy of CP desorption from PACP suggests that the CP converted to hydrates was contained in the large pores of the PACP. It is interesting to note that salinity had no significant impact on the degree of thermal energy compensation obtained.

Keywords: CP hydrates; CP-adsorption/desorption; activated carbon; energy compensation; hydrate-based processes; desalination

1. Introduction

Hydrate-based desalination (HBD) is a potential water-desalination technology that was first proposed by A. Parker in 1942 [1] and has received marked attention since the 1960s in order to strengthen the water-energy nexus [2]. It is based on the formation of gas hydrates which, once formed, are separated and dissociated to obtain desalinated water due to the fact that salt ions do not participate in the hydrate structure [3]. Gas hydrates are ice-like compounds formed by the association of water cages and small chemical compounds known as guests. They generally form at relatively high pressures and low temperatures [4]. Some of them, such as cyclopentane (CP) hydrates, can however form at atmospheric pressure. Hydrate crystallization has been widely studied in the literature in different contexts such as natural sediments [5–7], flow assurance [8–10] and hydrate-based processes [2,3,11–15]. A significant number of water-guest systems and experimental set-up designs have been studied, mainly to describe hydrate formation mechanisms [16,17] or hydrate crystal morphology [18–

20], to promote [21,22] or inhibit [8,23] hydrate formation, and to reduce the energy required for hydrate crystallization [24–28]. The optimization of energy consumption for hydrate crystallization, which is an exothermic reaction, has essentially been studied in the context of an economically viable hydrate-based desalination process. In the studies published, the authors generally tried to make the most of the endothermic energy produced by a reaction which is exogenous to the system. For instance, He et al. (2018) and Babu et al. (2020) attempted to make use of LNG regasification to cool the water to be desalinated [24,25]. He et al. (2018) achieved a decrease in specific energy consumption of 27.42% and 24.61% for 3.5wt% NaCl and 7 wt% NaCl brines respectively [25].

The hydrate formation stage of a recently patented HBD process [29], which has the particularity to use porous activated carbon particles (PACP) loaded with CP, was studied in a previous paper [22]. The main results showed that the PACP act as both kinetic promoters and a source of CP for hydrate formation. However, a relatively small amount of hydrates was obtained (< 50% of the theoretical maximum amount of hydrates that could be formed) [22]. This was proven to be related to the fact that the CP found in the small pores of the PACP remains trapped [30,31]. Based on this observation, PACP with predominantly large pores were recommended for enhancing the process. In the present work, we focus on the energy aspect of the hydrate formation stage in this HBD process, in which the energy supplied by hydrate crystallization - exothermic reaction (-115.4 kJ/mol of CP [32]) - could possibly be partially compensated by a reaction endogenous to the system, namely the desorption of CP from the PACP, which is endothermic (+28 to +57 kJ/mole of CP [30]).

The main objective of the present work is to experimentally prove this partial thermal energy compensation and determine its value. To do so, CP hydrates were crystallized from CP-saturated PACP immersed in brines of 3.5 wt% NaCl and 8 wt% NaCl, at a subcooling (difference between the hydrate equilibrium temperature and the experiment temperature) of

6°C. These salt concentrations mimic those of seawater [33] and produced water [11] respectively. The experiments were carried out using both differential scanning calorimetry (DSC) and refractive index measurements.

2. Experimental section

2.1. Materials and Apparatus

CP (purity of 97%) was supplied by Sigma Aldrich. Deionized water (resistivity of 18.2 MΩ.cm) was produced by a Purelab laboratory water-purification system. Sodium chloride (NaCl) (purity of 99.5%) was purchased from Acros Organics. A grade of PACP called BGX, supplied by Chemviron SA (Belgium), was used for the hydrate formation experiments. BGX is granular activated carbon with an average particle size of about 1 mm and a pore size distribution that has the specificity of being developed in both the meso- and macroporous regions in addition to the more standard microporous range (see SM-1 and SM-2). Their CP-adsorption capacity is 0.96 ± 0.02 g of CP/g of BGX at 1°C (see SM-3). A closed vessel and a set of resealable glass flasks with a 5-ml capacity were used for the CP-saturated PACP preparation. Plastic syringes (3-mL capacity) and cellulose acetate syringe filters (0.8-µm mesh size), used to sample and filter the unconverted water at the end of the hydrate formation experiments, were purchased from Sodipro.

A vacuum preparation apparatus called VacPrep™ (from Micromeritics) was used to purify the PACP samples under primary vacuum at 200°C. The samples were weighed using an ALC-110.4 balance (from Accurlab ®) with an uncertainty of 10^{-4} g. A universal convection incubator (from Memmert®) was used to impose the chosen temperature on the closed vessel,

in which the PACP are placed to be saturated with CP (cf. paragraph 2.2.). Hydrate formation was performed in the measurement cell (7-cm^3 capacity) of a Tian-Calvet BT2.15 calorimeter (from Setaram Instrumentation). The uncertainty with regard to the measured energy is 4% (see SM-4).

The refractive index nD (at a wavelength of 589.3 nm) of the water samples was measured using an Abbemat 550 refractometer (from Anton Paar) with an accuracy of ± 0.00001.

2.2. Preparation of the CP-saturated PACP

The saturation of PACP with CP was performed as follows: 0.54 g of BGX were purified at 200°C under primary vacuum for 12 hrs. Using a glass funnel, 0.500 ± 0.005 g of this hot sample was immediately transferred to a resealable glass flask, which was then introduced into the closed vessel partially filled with liquid CP (Fig. 1). This in turn was placed in the incubator at 1.0 ± 0.5°C. The PACP were left in contact with saturating CP vapor for 48 hrs to saturate their pores with CP.

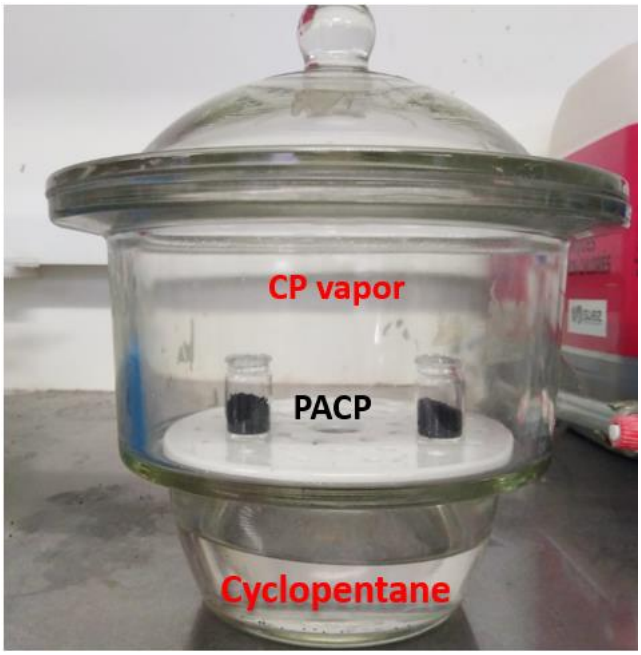

Fig. 1. Preparation of CP-saturated PACP

2.3. Investigation into the CP desorption-CP hydrate crystallization thermal energy compensation

CP hydrates were formed in systems composed of CP-saturated BGX immersed in brine (3.5 wt% NaCl and 8 wt% NaCl). In order to evaluate whether or not the thermal energy consumed by CP desorption from the PACP partially compensates the thermal energy released by hydrate crystallization, the thermal energy compensation was assessed by comparing the thermal energy measured in the DSC hydrate formation experiments (referred to as direct measurement) with the value deduced from the refractive index measurements of the unconverted water sampled at the end of the hydrate formation experiments (referred to as indirect measurement). The former corresponds to the energy $E_{des+crys}$ generated by CP-desorption and hydrate crystallization, whereas the latter corresponds to the energy E_{crys} generated by hydrate crystallization only.

For this experiment, 0.500 ± 0.005 g of CP-saturated BGX and 4.15 g (or 4.35 g) of 3.5 wt% NaCl (or 8 wt% NaCl) solution were introduced into the measurement cell of the BT2.15 calorimeter along with a few CP-hydrate crystals prepared beforehand (see Fig.2). These hydrate crystals were added to initiate hydrate crystallization by using the so called "memory effect". Memory effect is a phenomenon resulting from the non-complete dissociation of hydrate structure which reduces the time required to initiate hydrate formation [4]. The PACP, NaCl solution and cell were all precooled to the equilibrium temperature T_{eq} (5.5°C and 2.8°C for the 3.5 wt% NaCl and 8 wt% NaCl solutions respectively [22]). The cell was then introduced into the calorimeter, which was set at a temperature 0.2°C above T_{eq} in order to prevent (or at least limit) the added hydrate crystals from melting. The system was maintained at this temperature for one hour (stage (a) in Fig. 3) so that the thermal signal (heat flow) caused by the introduction of the cell into the calorimeter should reach the baseline and the added hydrate crystals should melt slowly. Then, the system temperature was decreased to the target temperature (T_{eq} – 6°C), at a cooling rate of 1°C/min, and maintained for 24 hrs (stage (b)). After 24 hrs of hydrate formation, the cell was removed from the calorimeter, a sample of the residual (unconverted) NaCl solution was collected and filtered, and its refractive index was measured (stage (c)).

$E_{des+crys}$, deduced from the direct measurements, was obtained by integrating the thermal peak generated by subtracting the "blank" thermogram (obtained in a similar fashion but without CP) from the "experiment" one (see Fig. 4). The "blank" thermogram (brown curve in Fig. 4) only takes into account the heat flow deviations due to the temperature programming and mass difference between the "measurement" and "reference" cells. Thus, the resulting thermogram "Experiment minus Blank" (blue curve in Fig. 4) only shows the heat flows due to both the CP desorption from the PACP and the hydrate crystallization, and its integration gives $E_{des+crys}$.

158 E_{crys}, deduced from the indirect measurements, was obtained by first determining the salinity
159 $[NaCl]_{24h}$ of the unconverted solution - concentrated with salt as hydrates formed - from the
160 measured refractive index and a previously generated "nD-[NaCl]" calibration curve (see SM-
161 5). Based on this, the water-to-hydrate conversion (WHC) and the water-to-hydrate amount
162 (WHA) were determined using equations 1 and 2 respectively. The stoichiometric ratio of CP
163 to water in the CP hydrates (1 mole of CP:17 moles of water) served to determine the amount
164 of CP-to-hydrates obtained (CPHA) (equation 3). The hydrate formation energy was deduced
165 from the CP-hydrate dissociation enthalpy (115,400 ± 7,600 J/mole of CP (Delroisse et al.,
166 2018)) using equation 4.

167 $$WHC(\%) = 100 - \frac{100*[NaCl]_i*(100-[NaCl]_{24h})}{(100-[NaCl]_i)*[NaCl]_{24h}} \quad (1)$$

168 $$WHA\ (g) = m_{iw} * WHC\ (\%) \quad (2)$$

169 where $[NaCl]_i$, $[NaCl]_{24h}$ and m_{iw} are the initial water salinity (3.5 wt% NaCl or 8 wt%
170 NaCl), the final water salinity (after 24 hrs.) and the initial pure-water mass respectively.

171 $$CPHA\ (g) = \frac{WHA*(17*18)}{70.13} \quad (3)$$

172 $$E_{crys}\ (J) = \frac{CPHA*115400}{70.13} \quad (4)$$

173 The uncertainties as regards $E_{des+crys}$ were determined as the sum of experiment repetition
174 and calibration-control deviations, whereas the uncertainties as regards E_{crys} were calculated
175 from the experiment-repetition deviation, the calibration curve deviation, the refractometer
176 accuracy, and the uncertainty regarding the dissociation enthalpy.
177

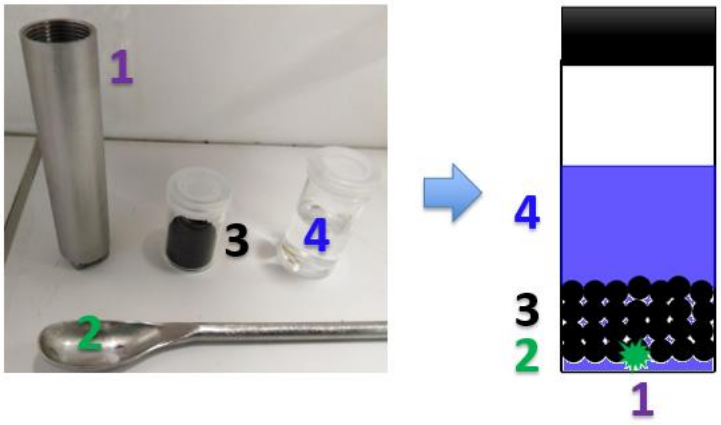

Fig. 2. Preparing the system for the hydrate formation experiment in the calorimetric cell of the BT2.15 apparatus. **1)** The measurement cell, **2)** hydrate seed, **3)** CP-saturated PACP, and **4)** brine

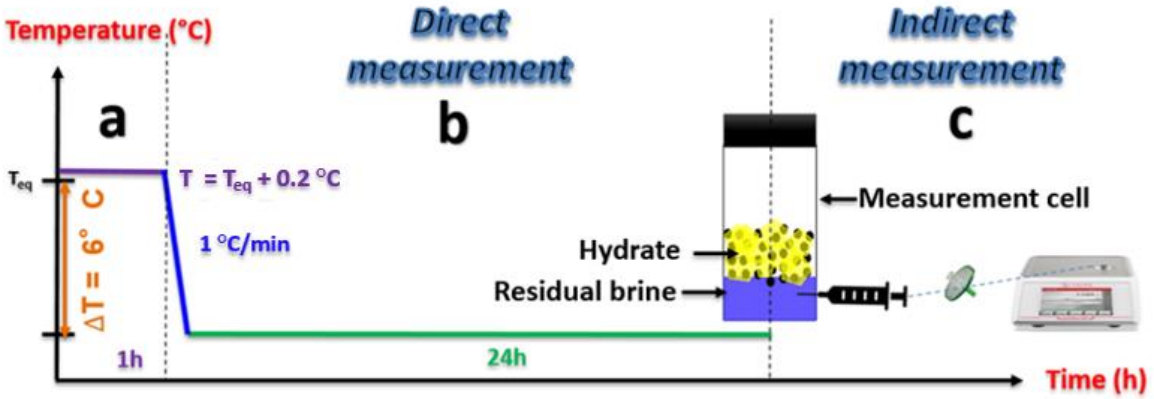

Fig. 3. Experimental procedure to determine thermal energy compensation

3. Results and discussion

Fig. 4 shows the resulting thermal peak (green curve) obtained after subtracting the "blank" thermogram (brown curve) from the "experiment" one (blue curve) for both NaCl solutions. The superposition of the thermal peaks obtained in experiments 1 and 2 shows a good

reproducibility for each salinity (Fig. 5). The average values of $E_{des+crys}$ obtained by integrating the thermal peaks are also given in Fig. 5.

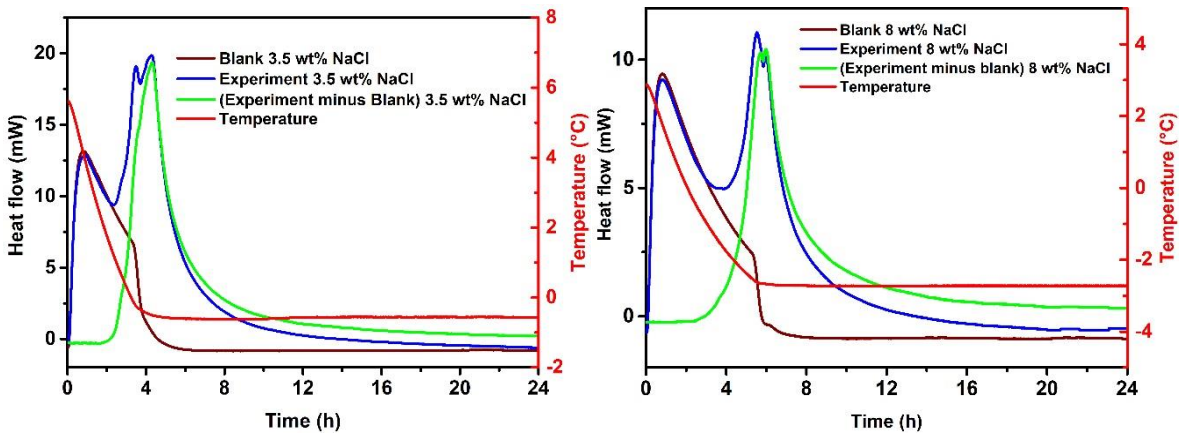

Fig. 4. Thermal energy peak (green curve) generated by subtracting the "blank" thermogram (brown curve) from the "experiment" thermogram (blue curve) for the 3.5 wt% NaCl solution (left) and 8 wt% NaCl solution (right)

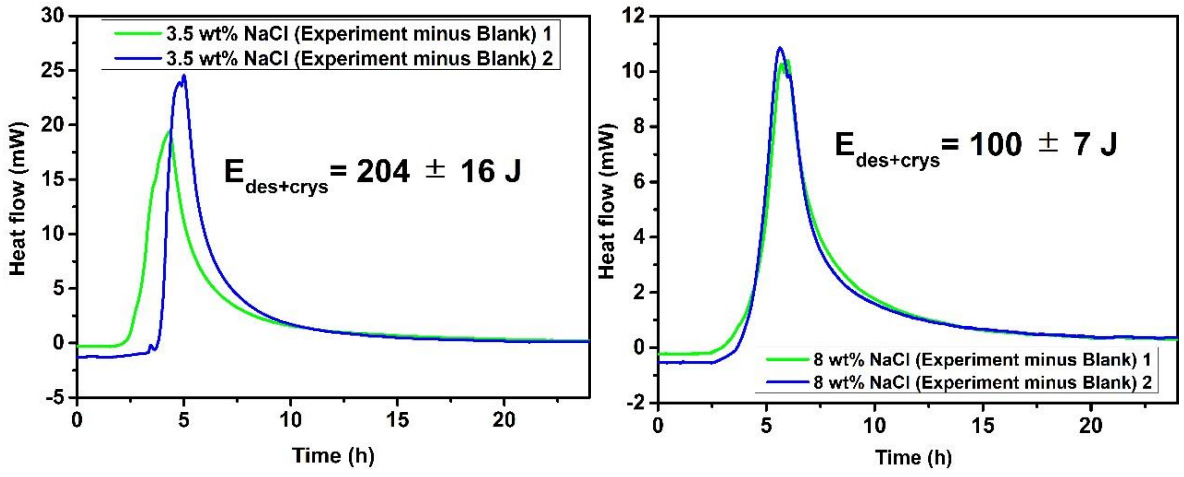

Fig. 5. Comparison of the thermal energy peak obtained in two repeated experiments with the 3.5 wt% NaCl solution (left) and the 8 wt% NaCl solution (right). The values of $E_{des+crys}$ were obtained by integrating the peaks.

The thermal energy values E_{crys} deduced from the indirect measurements for the same systems are given in Table 1. The refractive indexes (nD) measured after 24 hrs of hydrate formation in experiments 1 and 2 are in good agreement which indicates a good reproducibility (difference of less than 0.002%).

Table 1. Indirect measurement of hydrate formation energy

		3.5 wt% NaCl	8 wt% NaCl
nD	Exp. 1	1.340402	1.348213
at t = 24 h	Exp. 2	1.340376	1.348220
	Average	1.340390 ± 0.00001	1.34822 ± 0.00001
$[NaCl]_{24h}$ (wt%)		4.23 ± 0.01	8.71 ± 0.01
WHC (%)		18.0 ± 0.4	8.70 ± 0.25
WHA (g)		0.72 ± 0.02	0.35 ± 0.01
CPHA (g)		0.160 ± 0.004	0.080 ± 0.002
E_{crys} (J)		271 ± 24	131 ± 12

As can be seen in Table 2, $E_{des+crys}$ is lower than E_{crys}. The difference in energy ($E_{crys} - E_{des+crys}$) is in fact the balanced energy. Since the PACP are initially saturated with CP, meaning that the CP is found only within the pores, the balanced energy can thus be fully attributed to CP desorption. While assuming that all the CP desorbed from the PACP is converted to hydrates (i.e. the desorbed-CP amount is equal to CPHA), the balanced energy value, calculated as the ratio of ($E_{crys} - E_{des+crys}$) to CPHA (in mol), is between 9 (=28-19) kJ/mol of CP and 47 (=28+19) kJ/mol of CP. The balanced energy can be compared to the differential enthalpy of CP desorption (the opposite of the differential enthalpy of CP adsorption on PACP), which ranges from 28 to 57 kJ/mol of CP. The differential enthalpy of

CP desorption was measured in a previous paper for two different activated carbons (see SM-6) [30] using the calorimetric-manometric technique [34]. The similarity of the curves indicates a general range of values for CP adsorbed on an activated carbon. For the sake of comparison, the balanced energy range and the differential enthalpy of CP desorption from PACP are plotted in the same figure (Fig. 6).

Table 2. Determination of the balanced energy per mole of CP

	3.5 wt% NaCl	8 wt% NaCl
$E_{des+crys}$ (J)	204 ± 16	100 ± 7
E_{crys} (J)	271 ± 24	131 ± 12
CPHA (g)	0.16	0.08
	$(2.3\ 10^{-3})^*$	$(1.1\ 10^{-3})^*$
Balanced energy (J)	67 ± 40	31 ± 19
Balanced energy (kJ/mol CP)	29 ± 17	28 ± 19

*value of CPHA in mol

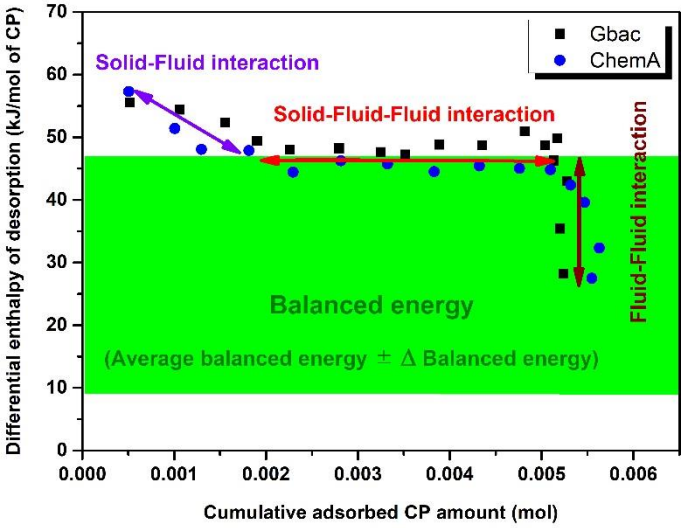

Fig. 6. Comparison of the balanced energy obtained in the case of hydrate formation from CP-saturated PACP (green area), and differential enthalpy of CP desorption from PACP (blue and black dots) [30]

As can be seen in Figure 6, the former (green area) does not cover the entire range of the latter (dots), which confirms that part of the CP did not desorb from the PACP (and therefore did not participate in the formation of hydrates). The high enthalpy values (48 to 57 kJ/mol of CP) of the uncovered dots correspond to the filling of pores at the lowest pressures ($0 < P_{eq}/P_{sat} <\sim 0.02$) [30] *i.e.* the smallest pores, mainly micropores, where the prevailing interactions are fluid-solid. The non-desorbed CP was therefore trapped in these pores. The enthalpy values of the covered dots (28 to 48 kJ/mol of CP) correspond to medium-to-high-pressure filling of the meso- and macropores ($\sim 0.02 < P_{eq}/P_{sat} < 1$) [30]. Hence, CP that desorbed from the PACP to form hydrates was contained in these pore ranges where the prevailing interactions are solid-fluid-fluid and fluid-fluid interactions. One can see that the balanced energy range obtained was almost the same for both salinities (3.5 wt% NaCl and 8 wt% NaCl), suggesting no significant effect of salt on this phenomenon. This result makes sense since the balanced energy was found to be related to the CP-desorption energy. The balanced energy (+9 to +47 kJ/mol of CP) implied a thermal energy compensation of between 8% and 40% of the energy supplied by hydrate crystallization. The (positive) balanced energy (+9 to +47 kJ/mol of CP) implied a thermal energy compensation of the (negative) energy supplied by the hydrate crystallization (-115.4 kJ/mol of CP). Its value, calculated as the ratio of the balanced energy to the dissociation enthalpy of CP hydrates, is between 8% (=100×9:115.4) and 40% (=100×47:115.4).

The investigation into the thermal energy compensation together with the assumption that (some) water molecules can enter the pores of PACP [16,31] lead us to propose a mechanism

for CP-hydrate formation from CP-saturated PACP (Fig. 7). In the smallest pores, the fluid-solid interactions prevent CP from desorbing and thus from participating in hydrate formation. In larger pores, the prevailing interactions (solid-fluid-fluid and fluid-fluid interactions) allow the desorption of CP (or at least part of it). In this case, hydrate formation can occur outside and/or inside the pore.

It should be noted that the surface chemistry of the PACP is reported to impact (promote or inhibit) hydrate crystallization [8,16,35]. However, in the case of our investigated system, the low-size pores of PACP, where the specific surface is significant and thus also the surface chemistry effects could be, do not participate to hydrate formation as previously explained. Therefore, the role of surface chemistry is probably not critical compared to that of pore size.

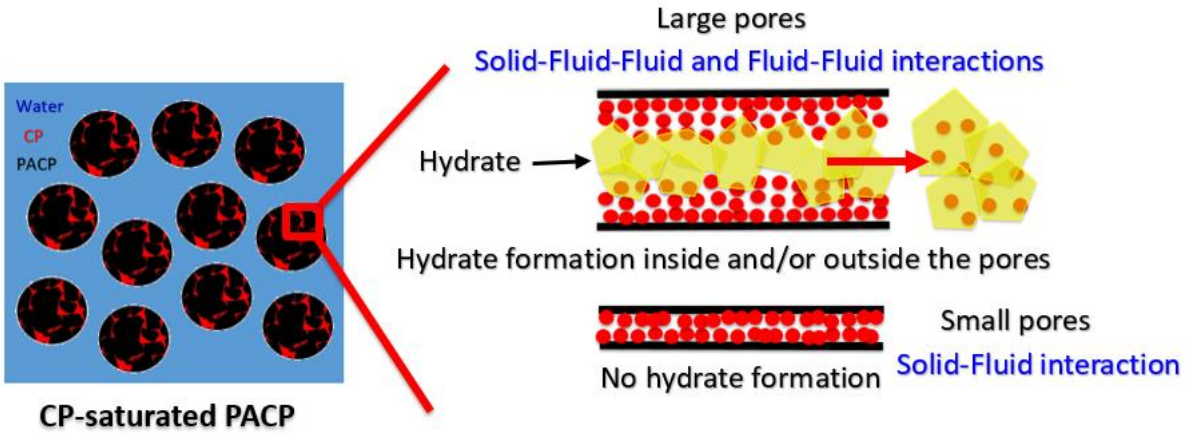

Fig. 7. Proposed prevailing mechanisms of hydrate formation from CP-saturated PACP immersed in water

4. Conclusions

In this work, the partial thermal energy compensation that may occur during hydrate formation from CP adsorbed in PACP was investigated in brines with salt concentrations typical of seawater (3.5 wt% NaCl) and produced water (8 wt% NaCl). A combination of differential scanning calorimetry and refractive index measurements were used to determine the thermal energies released by both the hydrate crystallization and CP desorption from the PACP ($E_{des+crys}$), and by the hydrate crystallization alone (E_{crys}). The balanced energy ($E_{crys} - E_{des+crys}$) was found to range between 9 and 47 kJ/mol of CP for both salinities, which means that it might be possible to save 8% to 40% of the energy required by hydrate crystallization in hydrate-based desalination processes. This energy can be attributed to the desorption of CP from the large pores of the PACP. This result demonstrates that the CP converted to hydrates was contained by the largest pores of the PACP, and that the part of CP adsorbed in the smallest ones remained trapped. In the light of these results, a mechanism of hydrate formation in these types of CP-saturated PACP has been proposed.

Acknowledgments

This research was financially supported by Total. The authors would like to thank Manuel Ildefonso (UPPA), Pascal Le Mélinaire (BGH), and Patrick Baldoni-Andrey, Hervé Nabet, and Stéphane Nowe (Total) for their valuable scientific inputs and discussions. C. Miqueu acknowledges the E2S UPPA hub Newpores supported by the "Investissements d'Avenir" French programme managed by ANR (ANR-16-IDEX-0002).

References

[1] Parker, A. Potable water from sea-water. Nature 1942. https://doi.org/DOI 10.1038/149184a0.

[2] Babu P, Nambiar A, He T, Karimi IA, Lee JD, Englezos P, et al. A Review of Clathrate Hydrate Based Desalination To Strengthen Energy–Water Nexus. ACS Sustain Chem Eng 2018;6:8093–107. https://doi.org/10.1021/acssuschemeng.8b01616.
[3] Zheng J, Cheng F, Li Y, Lü X, Yang M. Progress and trends in hydrate based desalination (HBD) technology: A review. Chin J Chem Eng 2019;27:2037–43. https://doi.org/10.1016/j.cjche.2019.02.017.
[4] Sloan, E. D.; Koh, C. A. Clathrate Hydrates of Natural Gases. Third Edition. CRC Press, Taylor & Francis Group, Boca Raton,; 2008.
[5] Tohidi B, Burgass RW, Danesh A, Østergaard KK, Todd AC. Improving the accuracy of gas hydrate dissociation point measurements. Ann N Y Acad Sci 2000;912:924–31. https://doi.org/10.1111/j.1749-6632.2000.tb06846.x.
[6] Atig D, Broseta D, Pereira J-M, Brown R. Contactless probing of polycrystalline methane hydrate at pore scale suggests weaker tensile properties than thought. Nat Commun 2020;11:3379. https://doi.org/10.1038/s41467-020-16628-4.
[7] Qanbari F, Pooladi-Darvish M, Hamed Tabatabaie S, Gerami S. Storage of CO2 as hydrate beneath the ocean floor. Energy Procedia 2011;4:3997–4004. https://doi.org/10.1016/j.egypro.2011.02.340.
[8] Baek S, Min J, Lee JW. Inhibition effects of activated carbon particles on gas hydrate formation at oil-water interfaces. RSC Adv 2015;5:58813–20. https://doi.org/10.1039/c5ra08335d.
[9] Liu W, Li X, Hu J, Wu K, Sun F, Sun Z, et al. Research on flow assurance of deepwater submarine natural gas pipelines: Hydrate prediction and prevention. J Loss Prev Process Ind 2019;61:130–46. https://doi.org/10.1016/j.jlp.2019.06.007.
[10] Olajire AA. Flow assurance issues in deep-water gas well testing and mitigation strategies with respect to gas hydrates deposition in flowlines—A review. J Mol Liq 2020;318:114203. https://doi.org/10.1016/j.molliq.2020.114203.
[11] Cha J-H, Seol Y. Increasing Gas Hydrate Formation Temperature for Desalination of High Salinity Produced Water with Secondary Guests. ACS Sustain Chem Eng 2013;1:1218–24. https://doi.org/10.1021/sc400160u.
[12] Fakharian H, Ganji H, Naderifar A. Desalination of high salinity produced water using natural gas hydrate. J Taiwan Inst Chem Eng 2017;72:157–62. https://doi.org/10.1016/j.jtice.2017.01.025.
[13] Ho-Van S, Bouillot B, Douzet J, Babakhani SM, Herri JM. Cyclopentane hydrates – A candidate for desalination? J Environ Chem Eng 2019;7:103359. https://doi.org/10.1016/j.jece.2019.103359.
[14] Hydrate Technology For Transporting Natural Gas 2003;16:8.
[15] Torré J-P, Dicharry C, Ricaurte M, Daniel-David D, Broseta D. CO2 capture by hydrate formation in quiescent conditions: In search of efficient kinetic additives. Energy Procedia 2011;4:621–8. https://doi.org/10.1016/j.egypro.2011.01.097.
[16] Nguyen NN, Galib M, Nguyen AV. Critical Review on Gas Hydrate Formation at Solid Surfaces and in Confined Spaces—Why and How Does Interfacial Regime Matter? Energy Fuels 2020;34:6751–60. https://doi.org/10.1021/acs.energyfuels.0c01291.
[17] Linga P, Clarke MA. A Review of Reactor Designs and Materials Employed for Increasing the Rate of Gas Hydrate Formation. Energy Fuels 2017;31:1–13. https://doi.org/10.1021/acs.energyfuels.6b02304.
[18] Babu P, Yee D, Linga P, Palmer A, Khoo BC, Tan TS, et al. Morphology of Methane Hydrate Formation in Porous Media. Energy Fuels 2013;27:3364–72. https://doi.org/10.1021/ef4004818.

[19] Delroisse H, Torré J-P, Dicharry C. Effect of a Hydrophilic Cationic Surfactant on Cyclopentane Hydrate Crystal Growth at the Water/Cyclopentane Interface. Cryst Growth Des 2017;17:5098–107. https://doi.org/10.1021/acs.cgd.7b00241.
[20] Linga P, Haligva C, Nam SC, Ripmeester JA, Englezos P. Gas Hydrate Formation in a Variable Volume Bed of Silica Sand Particles. Energy Fuels 2009;23:5496–507. https://doi.org/10.1021/ef900542m.
[21] Li F, Chen Z, Dong H, Shi C, Wang B, Yang L, et al. Promotion effect of graphite on cyclopentane hydrate based desalination. Desalination 2018;445:197–203. https://doi.org/10.1016/j.desal.2018.08.011.
[22] Mallek R, Miqueu C, Jacob M, Le Mélinaire P, Dicharry C. Effect of porous activated carbon particles soaked in cyclopentane on CP-hydrate formation in synthetic produced water. J Water Process Eng 2020;38:101660. https://doi.org/10.1016/j.jwpe.2020.101660.
[23] Zylyftari G, Lee JW, Morris JF. Salt effects on thermodynamic and rheological properties of hydrate forming emulsions. Chem Eng Sci 2013;95:148–60. https://doi.org/10.1016/j.ces.2013.02.056.
[24] Babu P, Nambiar A, Chong ZR, Daraboina N, Albeirutty M, Bamaga OA, et al. Hydrate-based desalination (HyDesal) process employing a novel prototype design. Chem Eng Sci 2020;218:115563. https://doi.org/10.1016/j.ces.2020.115563.
[25] He T, Nair SK, Babu P, Linga P, Karimi IA. A novel conceptual design of hydrate based desalination (HyDesal) process by utilizing LNG cold energy. Appl Energy 2018;222:13–24. https://doi.org/10.1016/j.apenergy.2018.04.006.
[26] Chong ZR, He T, Babu P, Zheng J, Linga P. Economic evaluation of energy efficient hydrate based desalination utilizing cold energy from liquefied natural gas (LNG). Desalination 2019;463:69–80. https://doi.org/10.1016/j.desal.2019.04.015.
[27] Montazeri V, Rahimi M, Zarenezhad B. Energy saving in carbon dioxide hydrate formation process using Boehmite nanoparticles. Korean J Chem Eng 2019;36:1859–68. https://doi.org/10.1007/s11814-019-0375-y.
[28] Lee SH, Park K. Conceptual design and economic analysis of a novel cogeneration desalination process using LNG based on clathrate hydrate. Desalination 2021;498. https://doi.org/10.1016/j.desal.2020.114703.
[29] Method for crystallising clathrate hydrates, and method for purifying an aqueous liquid using the clathrate hydrates thus crystallised; Inventor: Bruno Mottet; Applicant: BGH[FR]. EP3153606, https://worldwide.espacenet.com/patent/search/family/054476876/publication/WO2017060456A1?q=PCT%2FEP2016%2F074044, n.d.
[30] Mallek R, Plantier F, Dicharry C, Jacob M, Miqueu C. Experimental characterization of cyclopentane adsorption/desorption in microporous activated carbons. Carbon Trends 2021;2:100021. https://doi.org/10.1016/j.cartre.2020.100021.
[31] R. Mallek, C. Miqueu, M. Jacob, C. Dicharry. Investigation on Cyclopentane-hydrate formation from CP-loaded porous activated carbon particles. Chemical engineering science,Submitted.
[32] Delroisse H, Plantier F, Marlin L, Dicharry C, Frouté L, André R, et al. Determination of thermophysical properties of cyclopentane hydrate using a stirred calorimetric cell. J Chem Thermodyn 2018;125:136–41. https://doi.org/10.1016/j.jct.2018.05.023.
[33] Kang KC, Linga P, Park K, Choi S-J, Lee JD. Seawater desalination by gas hydrate process and removal characteristics of dissolved ions (Na+, K+, Mg2+, Ca2+, B3+, Cl−, SO42−). Desalination 2014;353:84–90. https://doi.org/10.1016/j.desal.2014.09.007.
[34] Adil Mouahid. Mise au point point d'un dispositif couple manométrique calorimétrique pour l'étude de l'adsorption de fluides supercritiques dans des milieux microporeux et

mesoporeux. Physique[physics]. Université de Pau et des Pays de l'Adour., 2010. Francais. NNT : 10PAUU3020. tel-00573997. n.d.
[35] Ling Z, Shi C, Li F, Fu Y, Zhao J, Dong H, et al. Desalination and Li+ enrichment via formation of cyclopentane hydrate. Sep Purif Technol 2020;231:115921. https://doi.org/10.1016/j.seppur.2019.115921.

Supplementary Material

SM-1

Fig. S1. PSD and cumulative PV determined using gas porosimetry (Ar isotherms at 87K on Quantachrome IQ)

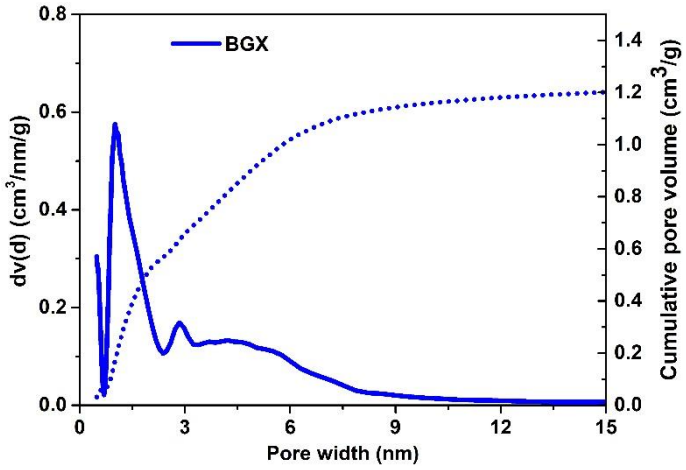

SM-2

Fig. S2. cumulative PV determined using mercury intrusion porosimetry (Micromeritics Autopore IV)

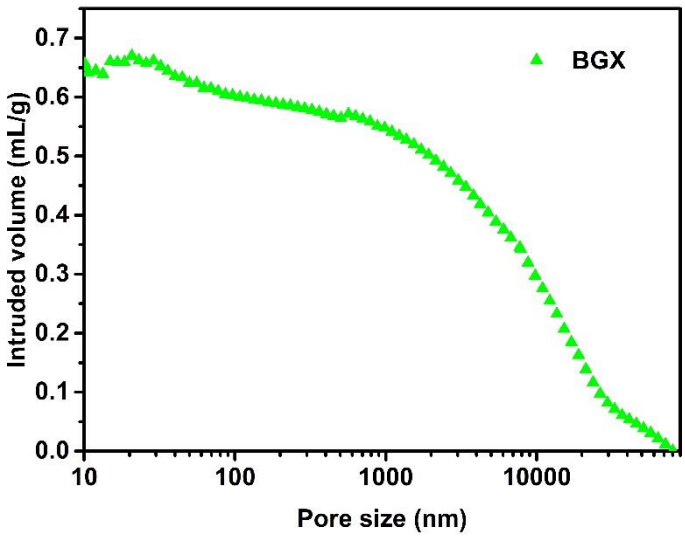

SM-3

Determination of the CP-adsorption capacity of BGX

To perform CP-adsorption capacity measurements, the PACP were purified at 200°C for 12 hrs under primary vacuum. Using a glass funnel, the hot purified sample was directly transferred into a small closable flask (5-mL capacity), which was then weighed and introduced into the CP adsorption chamber (closed-vessel partially filled with a flask of liquid CP). The PACP were only in contact with CP vapor (cf. Figure S1). The CP adsorption chamber was placed in the incubator at 1.0 ± 0.5°C. After 48 hrs of adsorption, the flask was weighed again and the CP-adsorption capacity of the PACP was determined. The experiment was repeated 3 times to check the results.

SM-4

Fig. S3. dissociation of ice used to determine the uncertainties associated with the DSC measurements

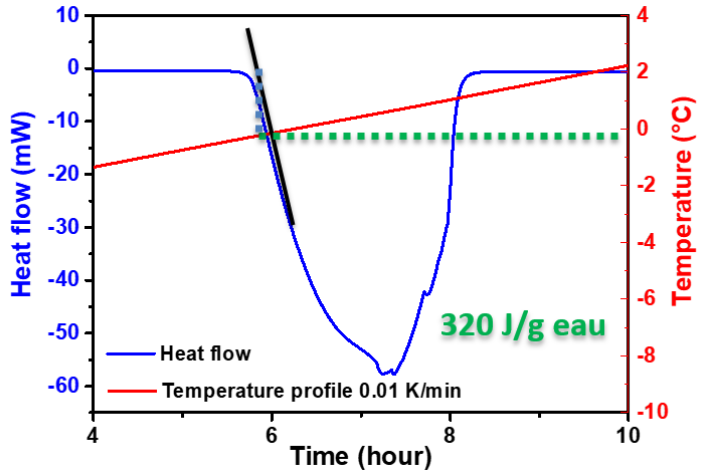

SM-5

Fig. S4. [NaCl]-nD calibration curve

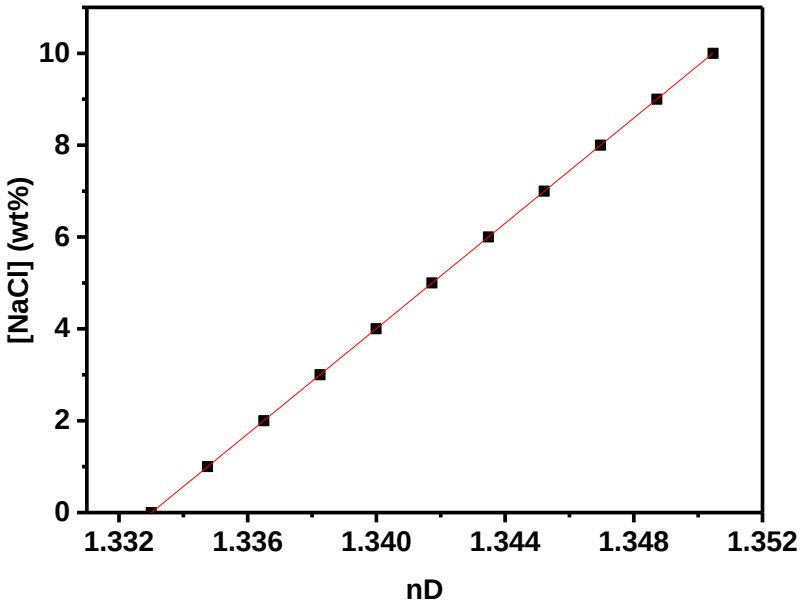

The calibration curve [NaCl] vs. nD was obtained by measuring the refractive index (nD) of previously prepared NaCl solutions of known concentrations [NaCl]. The linear regression of the [NaCl] vs the nD plot gave the following equation: [NaCl] = 573.044×nD – 763.87. The uncertainties regarding the slope and the offset were determined using the DROITEREG

function method (Δa = 0.18704; Δb=0.25096). The uncertainties Δ[NaCl] and ΔWHC regarding the salinity determined and the water-to-hydrate conversion (WHC) respectively, were obtained by differentiating the calibration equation and equation 1. Finally, ΔE_{crys} was obtained in a similar fashion after determining ΔWHA, ΔCPHA from the differentiation of equations 2 and 3.

SM-6

Gbac and ChemA are the notation used for G-BAC-G70R and Chemviron-A, which are two different PACP manufactured by Keruha Gmbh and Calgon, respectively. The differential enthalpies of CP-adsorption on these PACP were measured in a previous work [30], and they showed almost the same values despite their different origins and characteristics. The similarity of the obtained results indicates a general range of values for CP adsorption on activated carbons.

Table S1. Origin and characteristics of Gbac and ChemA

	Gbac	ChemA
Origin	Petroleum pitch	Coconut
Particle size (µm)	700	<177
Principal pore size (nm)	5.5 ; 0.79	5.5 ; 0.79; 1.3